Climatic Change
DOI 10.1007/s10584-012-0566-6

Effects of projected climate change on the hydrology in the Mono Lake Basin, California

Darren L. Ficklin · Iris T. Stewart · Edwin P. Maurer

Received: 29 August 2011 / Accepted: 28 July 2012

Abstract The Californian Mono Lake Basin (MLB) is a fragile ecosystem, for which a 1983 ruling carefully balanced water diversions with ecological needs without the consideration of global climate change. The hydroclimatologic response to the impact of projected climatic changes in the MLB has not been comprehensively assessed and is the focus of this study. Downscaled temperature and precipitation projections from 16 Global Climate Models (GCMs), using two emission scenarios (B1 and A2), were used to drive a calibrated Soil and Water Assessment Tool (SWAT) hydrologic model to assess the effects on streamflow on the two significant inflows to the MLB, Lee Vining and Rush Creeks. For the MLB, the GCM ensemble output suggests significant increases in annual temperature, averaging 2.5 and 4.1 °C for the B1 and A2 emission scenarios, respectively, with concurrent small (1–3 %) decreases in annual precipitation by the end of the century. Annual total evapotranspiration is projected to increase by 10 mm by the end of the century for both emission scenarios. SWAT modeling results suggest a significant hydrologic response in the MLB by the end of the century that includes a) decreases in annual streamflow by 15 % compared to historical conditions b) an advance of the peak snowmelt runoff to 1 month earlier (June to May), c) a decreased (10–15 %) occurrence of 'wet' hydrologic years, and d) and more frequent (7–22 %) drought conditions. Ecosystem health and water diversions may be affected by reduced water availability in the MLB by the end of the century.

1 Introduction

Mono Lake in the Californian Sierra Nevada is the preeminent icon of the water use struggle in the Western United States. Since the 1940s two of the three major tributaries flowing into Mono Lake have been diverted for water and power for the city of Los Angeles, California.

This article is part of a Special Issue on *"Climate Change and Water Resources in the Sierra Nevada"* edited by Robert Coats, Iris Stewart, and Constance Millar.

D. L. Ficklin (✉) · I. T. Stewart
Environmental Studies Institute, Santa Clara University, Santa Clara, CA 95053, USA
e-mail: dficklin@scu.edu

E. P. Maurer
Civil Engineering Department, Santa Clara University, Santa Clara, CA 95053, USA

Published online: 25 August 2012

Between 1941 and 1985 the Los Angeles Department of Water and Power (DWP) diverted an average of 84 million cubic meters per year out of Mono Lake Basin (MLB; Blumm and Schwartz 2003). In 1969, the diversions increased to 111 million cubic meters per year, consisting of approximately 17 % of Los Angeles' water supply (Steinhart 1980). Deprived of its major freshwater source, Mono Lake water level dropped by 11.2 m below the 1940 lake elevation (1,955.9 m above sea level) and lake volume shrunk by 45 % (Vorster 1985). This resulted in several major environmental problems: Mono Lake salinity concentration doubled; important nesting islands within the lake became peninsulas vulnerable for predation; photosynthetic rates of algae were drastically reduced; the reproductive abilities of brine shrimp became impaired; stream ecosystems were damages due to lack of streamflow; and air quality became poor because of the exposed lakebed (Steinhart 1980; Dana and Lenz 1986; Loomis 1987; Mono Basin EIR 1993).

Environmental communities and organizations such as the National Audubon Society and the Mono Lake Committee began to pay attention to these environmental problems. In 1979, these organizations filed a suit to control the DWP's diversions and after numerous procedural maneuverings, the California Supreme Court handed down its landmark decision in December 1983, that the public trust doctrine applied to Mono Lake. The Court ruled that the California State Water Resources Control Board (SWRCB) has the authority to reexamine past water allocation decisions and the responsibility to protect the lakes environmental, recreational, and aesthetic values where feasible.

Based on examination of public trust resources, flows needed for aquatic species protection, and impacts of the decision on water available for municipal and power production for Los Angeles, the SWRCB concluded that the water rights licenses of Los Angeles should be amended in several aspects. These changes included the establishment of minimum instream flows for protection of aquatic ecosystems, which limits diversions during the wet and dry seasons based on whether the previous hydrologic year is a 'dry', 'normal', or 'wet' year. Therefore, the rate and amount of future diversions will largely depend on the future climatic and hydrologic conditions within the MLB; however, to the best of our knowledge, these have not previously been assessed.

The MLB represents an important and unique ecosystem for several species. The natural salinity of Mono Lake prevents it from being a major freshwater fishery. The salinity, however, provides a productive habitat for brine shrimp and flies. These food sources, in conjunction with the in-lake islands and inlets, provide an important habitat for nearly 100 species of birds (Dana and Lenz 1986; Loomis 1987; Mono Basin EIR 1993). Nearly 80 % of the State of California's population of California gulls nests within these habitats (Loomis 1987). Therefore, in addition to water resources, it is expected that climate change may also have an effect on ecosystems that rely on a healthy lake habitat.

The goal of this study then, is to investigate the effects of projected climatic changes on the hydrology in the MLB. We use the Soil and Water Assessment Tool (SWAT) hydrologic model coupled with statistically downscaled projections of 16 Global Climate Models (GCMs), each under a higher and lower greenhouse gas emission scenario, to model the Lee Vining and Rush Creek watersheds in the MLB. Specifically, we aim to address the following questions: [1] What are the projected changes in precipitation and temperature for Mono Lake Basin under high and lower greenhouse gas emission scenarios?, [2] What are the projected changes in streamflow due to climate change within the Mono Lake Basin?, and [3] Based on the California Supreme Court definition, what will be the distribution of future 'dry', 'normal', and 'wet' years under climatic changes? The last two questions carry serious implications related to the future of water resource diversions for Los Angeles, and concurrently the aquatic ecosystem health within the MLB.

2 Materials and methods

2.1 Study site

The MLB is located approximately 305 km east of San Francisco on the eastern edge of the Sierra Nevada mountain range and western edge of the Great Basin (Fig. 1). The size of the MLB is approximately 1,800 km^2. Surface water runoff and groundwater is derived from precipitation, and since the MLB is hydrologically closed, all surface and groundwater drain towards Mono Lake (Vorster 1985). Also, because the MLB is hydrologically closed, the lake volume is sensitive to changing inflows (and evaporation), expressing these historically as variability in lake level. On average, approximately 82 % of the annual total Mono Lake inflow is in the form of runoff (streamflow and groundwater input), with the other 18 % coming from precipitation (Vorster 1985). Of the annual total runoff, approximately 89 % is from Sierra Nevada snowmelt. This snowmelt drains into the three principal streams that contribute runoff to Mono Lake: Rush Creek (carries 53 % of total runoff), Lee Vining Creek (33 %), and Mill Creek (14 %) (LADWP 1995). These data result in an average annual runoff ratio (runoff/precipitation) of approximately 0.66. Lee Vining and Rush Creeks are the only water bodies diverted for Los Angeles water use and are therefore the only inflows that are assessed in this study.

The region's climate is characterized by a high altitude Mediterranean climate with large seasonal and annual temperature and precipitation variability. Average annual precipitation is approximately 64 cm (WRCC 2011; Fig. 2). Much of the precipitation occurs as winter snow, and varies considerably with elevation and distance from the Sierra Nevada crest with a strong orographic effect. Mean annual temperatures vary from below freezing to approximately 8 °C. Mean daily winter temperature is below freezing during the winter season

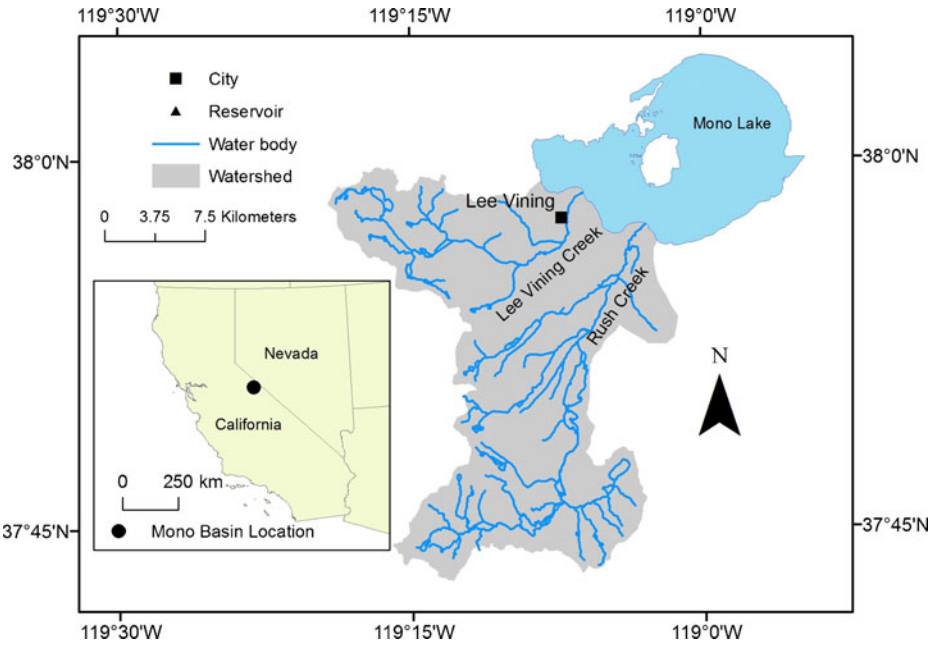

Fig. 1 California and the Mono Basin region, with the locations of Lee Vining and Rush Creeks

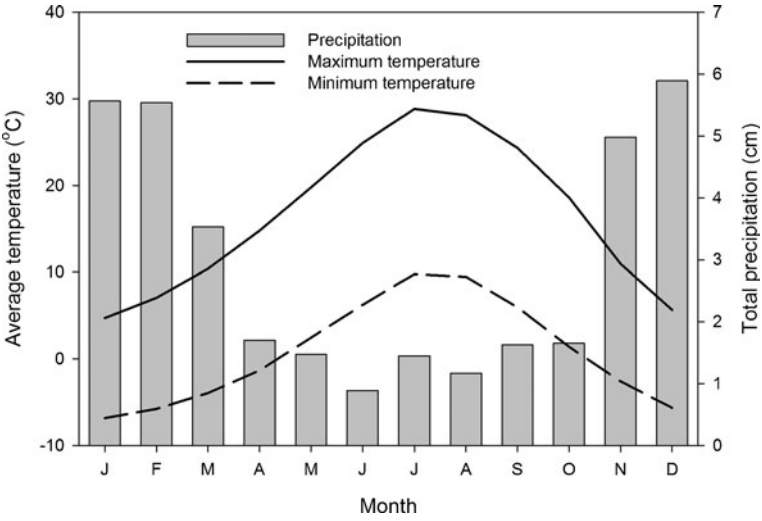

Fig. 2 Average monthly temperature and total precipitation in the Mono Lake Basin

(December through February), while the summer daily temperature is between 15.5 and 18.3 °C (WRCC 2011; Fig. 2). As a result, streamflow is highly seasonal, with most of the winter precipitation arriving as snowmelt-derived streamflow during the months of April through August.

2.2 Hydrologic model

SWAT is a continuous-time, quasi-physically based, distributed watershed model designed to simulate watershed processes at a river-basin scale (Arnold et al. 1998) and has been successfully applied in many settings (Gassman et al. 2007). SWAT models the entire hydrologic cycle, including surface flow, lateral flow, evapotranspiration, infiltration, deep percolation, and groundwater return flows. Input data for SWAT include basin topography, soil properties, land use/cover, and climate time-series data. The model was run at a monthly time step for 1950–1992 and future climate scenarios.

For this study, surface runoff was estimated using the Curve Number (CN; USDA 1972), and evapotranspiration was estimated using the Penman-Monteith method (Penman 1956; Monteith 1965). Water within the soil column can be removed by evaporation or plant water uptake, deep percolation for aquifer recharge, or move laterally in the soil column for streamflow contribution. Groundwater return flow is estimated based on the groundwater balance, where shallow and deep aquifers can contribute to streamflow. SWAT uses a temperature index-based approach to estimate snow accumulation and snowmelt processes within subbasin elevation bands based on the work of Fontaine et al. (2002). This study used four elevation bands for each subbasin. Further details on SWAT model components can be found in Neitsch et al. (2005).

2.3 Input data

SWAT input parameter values such as topography, land use/cover, and soils data were compiled using databases from various state and governmental agencies. A 30-m digital

elevation model (DEM) from the United States Geological Survey (USGS) was used for watershed and HRU delineation and the estimation of stream slopes. The 2001 National Land Cover database was used for land use/cover definition. This version was used because it is directly compatible with SWAT. The State Soil Geographic database (STATSGO) soil layer was used to derive the soil physical properties needed for SWAT. STATSGO was used over higher-resolution Soil Survey Geographic database (SSURGO) to decrease the computational requirements of the model and because of ease of use within SWAT. Natural flow data for Lee Vining and Rush Creek were gathered from the California Data Exchange Center (CDEC) and USGS. These data, which are estimated by the California Department of Water Resources (CA DWR), are derived from climate/runoff relationships and is the streamflow that would occur if no reservoirs were present. Daily climate data from 1949 to 1992, including precipitation, maximum and minimum temperature, and wind speed were obtained from gridded observed meteorological data (Maurer et al. 2002). The dataset is at a 1/8° (~12 km) spatial resolution. Solar radiation and relative humidity are generated for the historical and future scenarios using the built-in weather generator within SWAT. See Nietsch et al. (2005) for full weather generator details.

Projections from 16 GCMs in Table 1 using the emission scenarios of A2 (higher greenhouse gas emissions) and B1 (lower emissions) were used for climate change projections. Data include daily precipitation, maximum and minimum temperature, and wind speed from 1950 to 2099. All GCM data were obtained from World Climate Research

Table 1 Climate models used in the study

Model #	IPCC model ID	Modeling Group and Country	References
1	BCCR-BCM 2.0	Bjerknes Centre for Climate Research	Furevik et al. 2003
2	CGCM3.1 (T47)	Canadian Centre for Climate Modeling & Analysis	Flato and Boer 2001
3	CNRM-CM3	Météo-France/Centre National de Recherches Météorologiques, France	Salas-Mélia et al. 2005
4	CSIRO-Mk3.0	CSIRO Atmospheric Research, Australia	Gordon et al. 2002
5,6	GFDL-CM2: 2.0, 2.1	US Dept. of Commerce/NOAA/Geophysical Fluid Dynamics Laboratory, USA	Delworth et al. 2006
7	GISS-ER	NASA/Goddard Institute for Space Studies, USA	Russell and Rind 1999; Russell et al. 2000
8	INM-CM3.0	Institute for Numerical Mathematics, Russia	Diansky and Volodin 2002
9	IPSL-CM4	Institut Pierre Simon Laplace, France	IPSL 2005
10	MIROC3.2	Center for Climate System Research (The University of Tokyo), National Institute for Environmental Studies, and Frontier Research Center for Global Change (JAMSTEC), Japan	K-1 model developers 2004
11	ECHO-G	Meteorological Institute of the University of Bonn, Meteorological Research Institute of KMA	Legutke and Voss 1999
12	ECHAM5/MPI-OM	Max Planck Institute for Meteorology, Germany	Jungclaus et al. 2006
13	MRI-CGCM2.3.2	Meteorological Research Institute, Japan	Yukimoto et al. 2001
14	CCSM3	National Center for Atmospheric Research, USA	Collins et al. 2006
15	PCM	National Center for Atmospheric Research, USA	Washington et al. 2000
16	UKMO-HadCM3	Hadley Centre for Climate Prediction and Research/Met Office, UK	Gordon et al. 2000

Programme's (WCRP's) Coupled Model Intercomparison Project phase 3 (CMIP3) (Meehl et al. 2007a). All GCM output was then interpolated onto a common 2° grid, and statistically downscaled to 1/8° using the well-established bias-correction and spatial disaggregation (BCSD) method of Wood et al. (2002, 2004). The BCSD method has been widely applied in California and the western United States (e.g., Barnett et al. 2008; Cayan et al. 2008; Maurer 2007; Maurer et al. 2010). Wind data are randomly re-sampled historical wind data, where the same selected random month is used for precipitation, maximum temperature, minimum temperature and wind. The GCM output data are used to force SWAT to simulate the hydrologic response to future climate projections. The use of two emissions pathways and 16 GCMs ensures that the two most important sources of projection uncertainty for temperature and precipitation are assessed (Hawkins and Sutton 2009, 2010), namely the uncertainty associated with the level of GHGs and the response of the climate system to these increased GHG levels. While the uncertainties associated with the response of the climate to changes in atmospheric composition may be much larger than that represented by the ensemble of GCMs (Roe and Baker 2007; Sanderson et al. 2007), the use of ensembles of GCMs to characterize this is a common technique for assessing some of this uncertainty around the central tendency and to provide more quantitative climate change information for impacts studies (Meehl et al. 2007b).

2.4 SWAT model calibration and validation procedure

An automated calibration technique using the program Sequential Uncertainty Fitting Version 2 (SUFI-2; Abbaspour et al. 2007) was used to calibrate the SWAT model at the Lee Vining and Rush Creek outlets. Initial and default parameters relating to hydrology were varied until an optimal solution was met. Four optimization criteria were used: [1] the coefficient of determination (R^2), [2] a modified efficiency criterion ϕ (bR^2), [3] the Nash-Sutcliffe coefficient (NS), and [4] the mean square error (MSE). NS is defined as:

$$NS = 1 - \frac{\sum_{t=1}^{T} \left(Q_o^t - Q_m^t\right)^2}{\sum_{t=1}^{T} \left(Q_o^t - Q_o^{ave}\right)^2} \tag{2}$$

where NS is the Nash-Sutcliffe coefficient, Q_o^t is the observed data, Q_m^t is the simulated data, and Q_o^{ave} is the average of the observed data. A NS value of 1 is a perfect match of model data to observed data. ϕ is a slightly modified version of the efficiency criterion defined by Krause et al. (2005) where the coefficient of determination, R^2, is multiplied by the coefficient of the regression line between observed and simulated streamflows, b. This function allows accounting for the discrepancy in the magnitude of two signals (captured by b) as well as their dynamics (captured by R^2). ϕ is calculated by:

$$\phi = \begin{cases} |b|R^2 & if\ |b| \le 1 \\ |b|^{-1}R^2 & if\ |b| > 1 \end{cases} \tag{3}$$

For ϕ, a perfect simulation is represented by a value of 1. MSE is the mean of the square of the residuals between the observed and simulated data. The observed streamflow data from 1950 to 1974 was used as calibration, while the streamflow data from 1975 to 1992 was used for validation.

2.5 State Water Resource Control Board imposed in-stream requirements

For the protection of the lake and its ecosystem, the SWRCB decided on a set of streamflow flow rates to be met throughout the year based on whether the previous hydrologic year is 'wet', 'normal' or 'dry'(Table 2). The flows under this mandate must remain in the stream and shall not be diverted for any use. The hydrologic year (April 1st to March 31st) type is defined as:

- *Dry hydrologic conditions*: projected runoff of Lee Vining and Rush Creek less than 68.5 % of the 1950–1992 average
- *Normal hydrologic conditions*: projected runoff of Lee Vining and Rush Creek between 68.5 % and 136.5 % of the 1950–1992 average
- *Wet hydrologic conditions*: projected runoff of Lee Vining and Rush Creek greater than 136.5 % of the 1950–1992 average

The average SWAT-modeled monthly streamflow discharge for 1950–1992 is 3.06 m^3/s for Lee Vining and 2.04 m^3/s for Rush Creek, respectively. The hydrologic year streamflow flow rates for 'dry' and 'wet' conditions, which is based on the 1950–1992 SWAT-model average used in this study, can be found in Table 3.

2.6 Statistical analyses

T-tests for dependent samples were performed to compare all climate change and historical scenarios. The target level of significance was α=0.05.

3 Results and discussion

3.1 SWAT model calibration and validation

The SWAT simulation generated good results in the comparison with the unimpaired streamflow data at the Lee Vining and Rush Creek outlets (Fig. 3 and Table 4). At the Lee Vining site, the NS coefficient for streamflow was 0.86 for calibration and 0.81 for the validation period. The NS coefficient for the Rush Creek outlet was 0.82 and 0.79 for the calibration and validation period, respectively. The SWAT simulation also generated good seasonal results, with a NS value of 0.72 and 0.78 for the Spring and Summer months, respectively, for Lee Vining Creek and 0.59 and 0.90 for Rush Creek. Full calibration and validation

Table 2 In-stream streamflow requirements based on the California Supreme Court decision

Hydrologic year type	Season	Lee Vining Creek (m^3/s)	Rush Creek (m^3/s)
Dry	April 1 through September 30	1.05	0.88
	October 1 through March 31	0.71	1.02
Normal	April 1 through September 30	1.53	1.33
	October 1 through March 31	1.13	1.25
Wet	April 1 through September 30	1.53	1.93
	October 1 through March 31	1.13	1.47

Table 3 Streamflow values of 'wet' and 'dry' hydrologic year types

Site	Average (m^3/s)	Dry (m^3/s)	Wet (m^3/s)
Lee Vining Creek	2.04	<1.40	>2.80
Rush Creek	3.06	<2.10	>4.20

statistics can be found in Table 4. The SWAT simulations had the tendency to underestimate flows in the calibration period and overestimate flows in the validation period. This may be due to changes in land use, as the MLB has undergone a rapid conversion of rangeland for agricultural uses (USFWS 2006). The largest difference in the observed and simulated hydrographs occurs during the 1980s, where a large number of extremely wet years occurred (Karl and Riebsame 1984). These wet years largely led to an over-prediction compared to the observed data. Regardless, the calibration and validation results indicate satisfactory simulations based on the guidelines established by Moriasi et al. (2007), where a NS value greater than 0.50 is considered "satisfactory."

An analysis between streamflows simulated using observed climate data (from Maurer et al. 2002) and streamflows using historical GCM projections (1950–2010) was conducted to determine if there was a bias in the GCM projections. Overall, very little bias was found between the two historical streamflow sets for both emission scenarios. The NS coefficient between streamflow using observed climate and streamflow using historical B1 GCM projections was 0.98 for Lee Vining Creek and 0.98 for Rush Creek. Similar results were

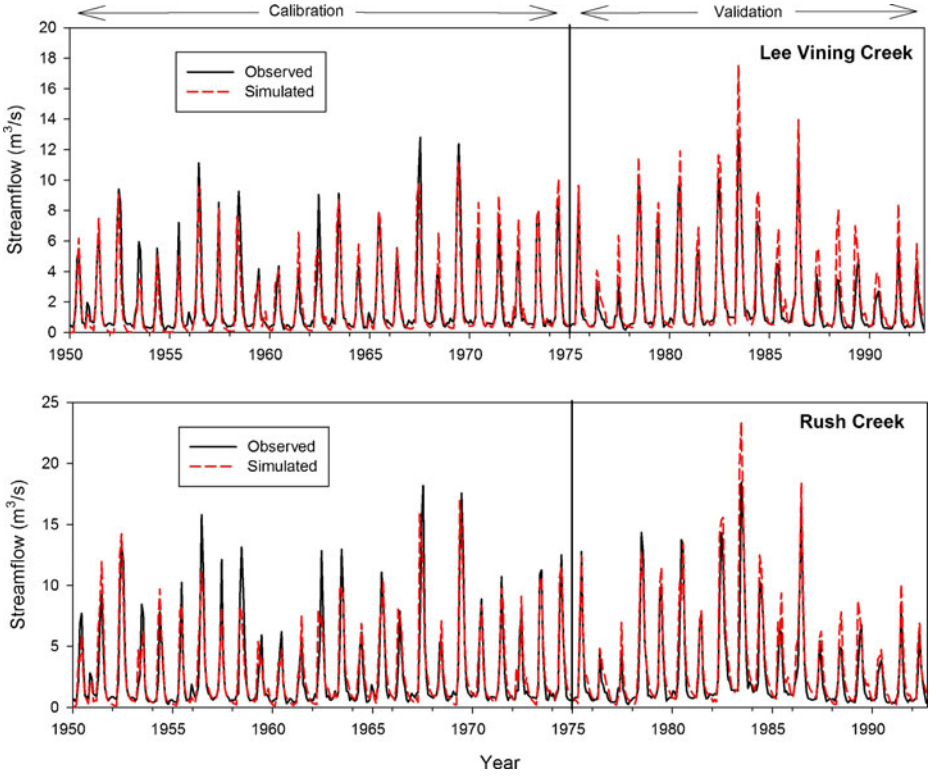

Fig. 3 Simulated and observed streamflow for the calibration and validation period at Lee Vining and Rush Creeks

Table 4 Model efficiency statistics for Lee Vining and Rush Creeks for the calibration and validation periods as well as all Spring and Summer months

	Calibration (1950–1974)				Validation (1975–1992)			
Site	R^2	NS	bR^2	MSE (m^3/s)	R^2	NS	bR^2	MSE (m^3/s)
Lee Vining Creek	0.86	0.86	0.79	0.83	0.91	0.81	0.78	1.12
Rush Creek	0.82	0.82	0.72	2.19	0.89	0.79	0.81	2.47
	Spring				Summer			
Lee Vining Creek	0.80	0.72	0.77	1.56	0.78	0.78	0.63	1.13
Rush Creek	0.67	0.59	0.55	2.68	0.87	0.90	0.71	1.05

found using the historical A2 GCM projections, where the NS coefficient was 0.99 for Lee Vining Creek and Rush Creek. The model efficiency statistic, percent bias, was also used to measure the tendency of the historical GCM projected streamflows to be larger or smaller than the observed climate simulated streamflows. The lower the value, the closer the datasets are to each other and a positive value indicate underestimation bias, while a negative value indicates overestimation bias. Comparing the streamflows simulated using observed climate and historical GCM projections, the percent biases for Lee Vining Creek was −6.6 % for the B1 emission scenario and 2.0 % for the A2 emission scenario. For Rush Creek, the percent biases were −9.1 % for the B1 emission scenario and −6.2 % for the A2 emission scenario. We therefore have confidence that the historical streamflows derived from GCM historical simulations are not significantly or systematically biased as compared to observed streamflow.

3.2 GCM projections for the Mono Lake Basin

Figures 4 and 5 show GCM projected changes in annual temperature and precipitation, respectively, between the historic (1961–1990) and future (2070–2099) periods for the 20 %, 50 % (median), and 80 % quantiles. According to the projections, the greatest warming is expected within the Sierra Nevada and east of the Sierra Nevada in the Great Basin. The median projection of temperature changes for the MLB range between 1.7 and 2.8 °C by the end of the century for the B1 emission scenario and 2.8 to 5.0 °C for the A2 emission scenario. For the 20 % quantile, the temperature change for the B1 and A2 scenarios is between 1.1 and 2.5 °C and 2.2 and 4.1 °C, respectively. For the 80 % quantile, the temperature change for the B1 and A2 scenarios is between 2.0 and 3.9 °C and 3.0 and 5.5 °C. The large variation in quantile temperature changes indicates a wide range in projected GCM temperature and precipitation estimates. Therefore, the use of all GCMs and emission scenarios in the analysis enables us to present results in terms of the inherent uncertainty of climate change projections.

The precipitation projections suggest a change, relative to 1961–1990, between −13 to 13.5 % for the B1 scenario and −16 to 16 % for the A2 scenario. Overall, the median precipitation suggests a slight but statistically insignificant ($p>0.05$) decrease over the MLB region. For the 20 % quantile, the precipitation changes range from −25.4 to 6.7 % for the B1 scenario and −34.7 to 11 % for the A2 scenario, with decreases in annual precipitation of approximately 15 % over the MLB region. The ranges for the 80 % quantile are −2 to 20 % and −5 to 38 % for the B1 and A2 scenarios, respectively, with increases in annual precipitation of approximately 8 % over the the MLB region.

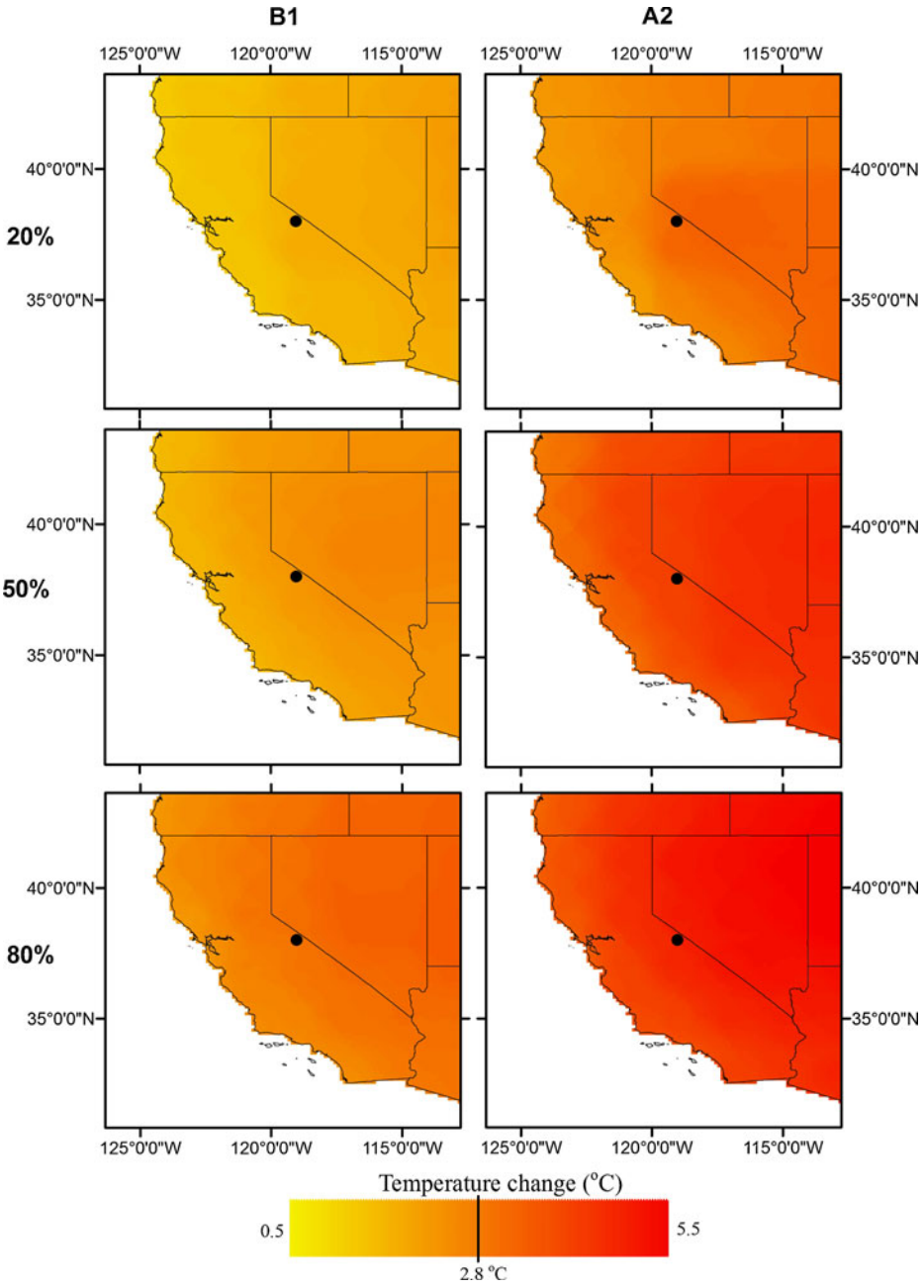

Fig. 4 Quantiles of the projected annual temperature change of the California region. The black circle represents the Mono Basin

Figure 6 shows the annual average change between the historic (1961–1990) and future (2070–2099) periods for each of the 16 GCMs under each emission scenario for the MLB. Annual increases in temperature average 2.5 and 4.0 °C for the B1 and A2 emission

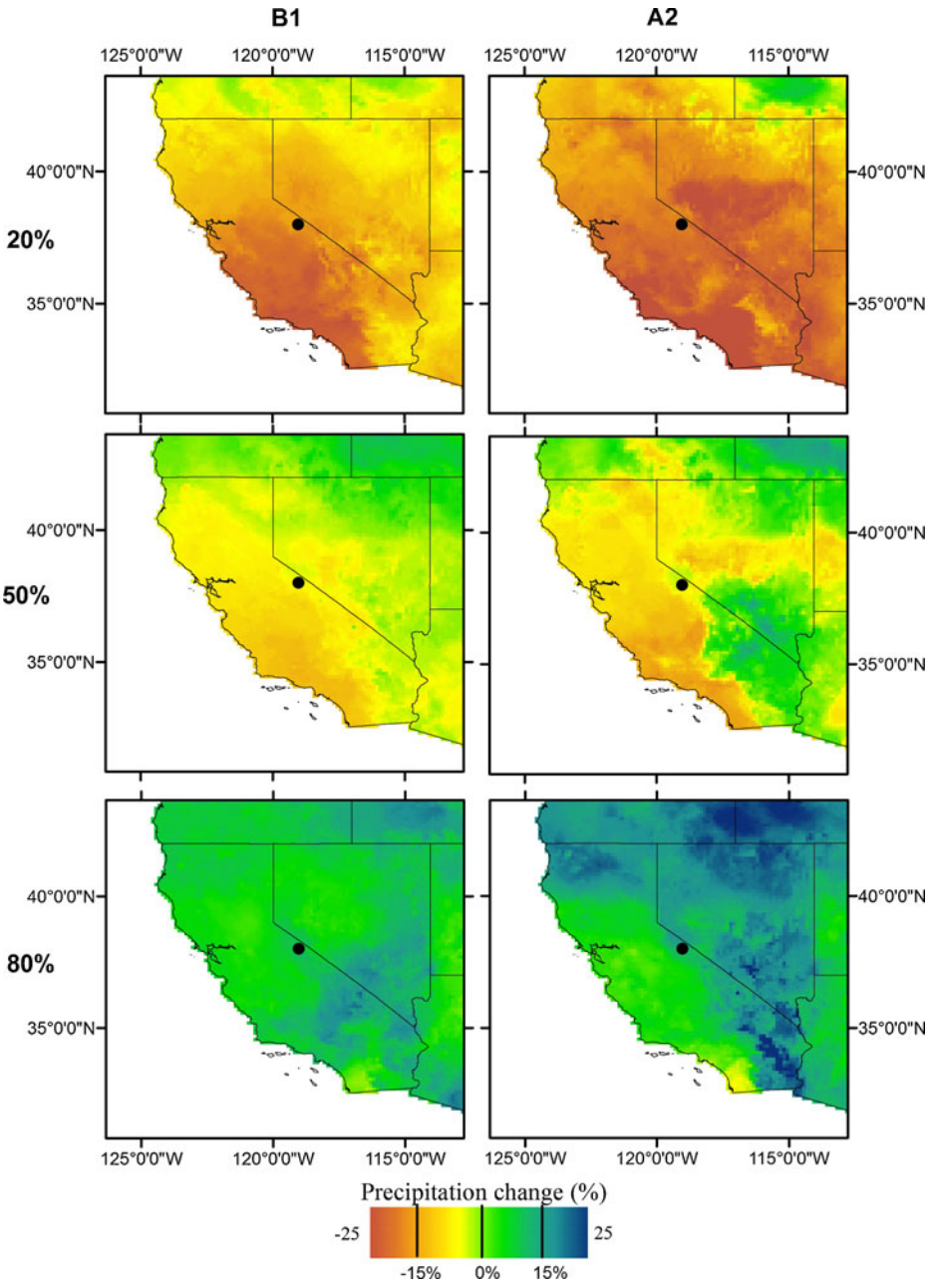

Fig. 5 Quantiles of the projected annual precipitation change of the California region. The black circle represents the Mono Basin

scenarios, respectively. Overall, 5 GCMs under the B1 emission scenario project a temperature increase greater than 2.8 °C, while 14 GCMs under the A2 emission scenario project an increase greater than 2.8 °C. All models suggest a warming of at least 1.7 °C for either emission scenario. The GCM ensemble projects a statistically insignificant ($p>0.05$)

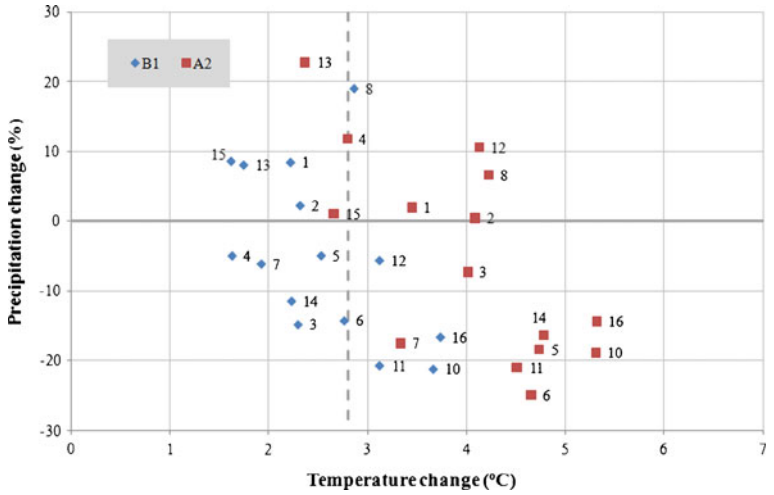

Fig. 6 End of the century change in temperature and precipitation for the 15 GCMs. The IPSL GCM is not plotted

decrease in annual precipitation by 3 % for the B1 scenario and 1.7 % for the A2 scenario. There was high variation in precipitation projections between GCMs, with a standard deviation of 14 % for the B1 scenario and 21 % for the A2 scenario. The Institute Pierre Simon Laplace (IPSL) GCM appears as an outlier regarding precipitation projections, showing an increase of 25.3 % for the B1 emission scenario and 56.9 % for the A2 emission scenario and is thus not plotted. When the IPSL GCM is removed from the ensemble, as has been done by others studying California with an ensemble of GCMs (Lobell et al. 2006), the ensemble mean average precipitation change, which is statistically insignificant ($p>0.05$) is −5 % for the B1 scenario and −6 % for the A2 scenario.

3.3 Future hydrology of the Mono Lake Basin

For the observed time period (1950–1992), SWAT was forced with daily observed climate data to assess its ability to reproduce historical Mono Lake inflows at the Lee Vining and Rush Creek outlets into the lake, as shown in Fig. 1. After calibration and validation, the SWAT model was then forced using daily data from 32 future climate projections (16 GCMs with two emission scenarios) through the end of the 21st century. The impact of potential climate change on streamflow was evaluated by comparing simulations using the GCMs in Table 1 under the B1 and A2 emission scenarios for two future time periods: 2050s (2040–2069) and 2080s (2070–2099) to those of the observed time period.

In California, evapotranspiration exerts a significant control on streamflow during the summer, where little to no precipitation occurs. Basin-wide total annual evapotranspiration is projected to increase under climate change. The historical annual total evaporanspiration for the MLB is 130.1 mm. Under the B1 scenario, evapotranspiration is projected to increase to 136.9 mm during the 2050s and 139.8 mm during the 2080s. Under the A2 scenario, larger end-of-the-century increases are expected, with increases to 135.7 mm during the 2050s and 140.7 mm during the 2080s. All increases are significant at the 0.05 level. With a projected decrease in precipitation, increased evapotranspiration may result in a large loss of water within the MLB.

At Lee Vining Creek, under the B1 emission scenario, annual streamflow (median of the GCM ensemble) is projected to decline by 0.24 (11 % decrease) and 0.30 m^3/s (13 %

decrease) for the 2050s and 2080s. Under the A2 scenario, annual streamflow is projected to decline by 0.11 m^3/s (5 % decrease) and 0.27 m^3/s (11 % decrease) for the 2050s and 2080s, respectively. Annual streamflow is projected to decrease for all time periods and scenarios for Rush Creek, with a 0.50 (15 % decrease) and 0.61 m^3/s (18 % decrease) decrease under the B1 emission scenario for the 2050s and 2080s, respectively, and a 0.32 (10 % decrease) and 0.63 m^3/s (19 % decrease) decrease under the A2 emission scenario for the 2050s and 2080s, respectively. The declines found for the 2050s were not significant at the 0.05 level, while the decline for the 2080s were significant at the 0.05 level. These results are consistent with the theory of Wigley and Jones (1985), where a median projection of a slight decline in precipitation would produce a more dramatic decrease in runoff when direct CO_2 effects are not modeled.

In addition to changes in annual runoff, streamflow timing is shifted as a result of earlier spring snowmelt, as shown in Figs. 7 and 8. Earlier spring snowmelt is due to higher spring temperatures, which results in a larger fraction of precipitation falling as rain rather than snow as well as earlier melt. Despite the large range of precipitation projections (Figs. 5 and 6), there was general agreement between GCMs that higher temperatures will lead to dramatic changes in the amount of snowfall and snowmelt-associated streamflow. For the historical time period,

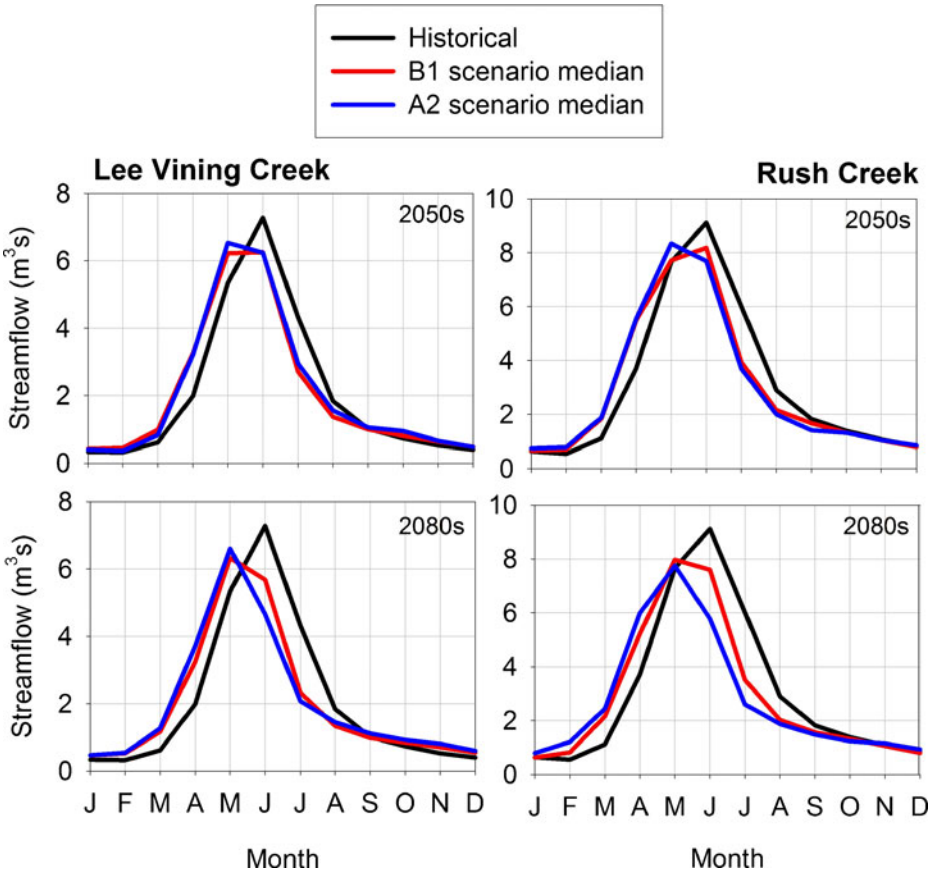

Fig. 7 Average monthly streamflow for the 2050s and 2080s under each emission scenario for Lee Vining and Rush Creeks

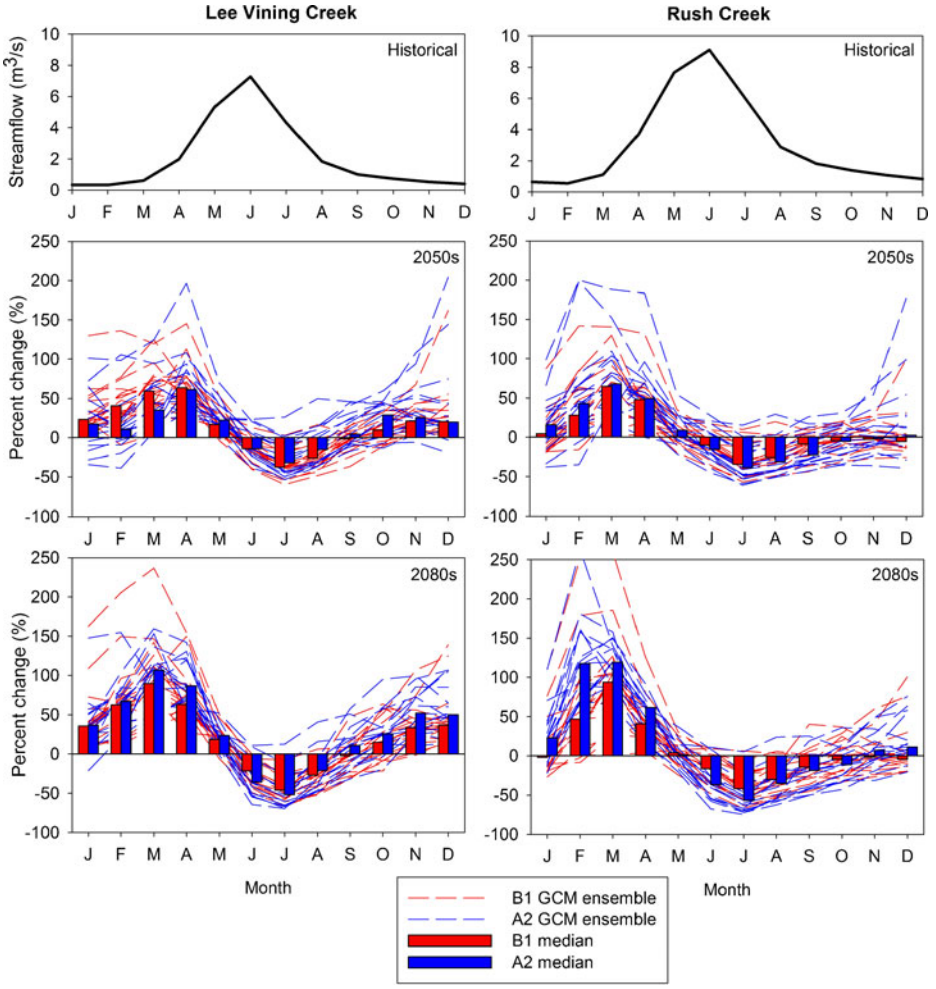

Fig. 8 Percent change in monthly streamflow for the 2050s and 2080s under each emission scenario for Lee Vining and Rush Creeks

the streamflows peaked in June, whereas, for the 2050s, streamflow peaked up to 1 month earlier, resulting in a June/May peak for the B1 emission scenario and a May peak for the A2 emission in Lee Vining and Rush Creeks. Further, the magnitude of the snowmelt peak decreased (Fig. 7). The accuracy of both the timing and the peak of the snowmelt runoff pulse are likely affected by the use of a monthly time step, however, earlier runoff timing and lower runoff peaks suggest a reduced snowmelt runoff volume. For the 2080s, under both emission scenarios, the timing of peak runoff was shifted by 1 month, from June to May. In addition, peak runoff decreased by 8 to 15 % for all future time periods and emission scenarios as compared to historical volumes.

Figure 8 illustrates that the GCM-driven simulations are in general agreement across models and emission scenarios in projecting winter and early spring streamflow increases and summer streamflow decreases. Thus water availability on the monthly scale will likely undergo significant changes. For Lee Vining Creek, average monthly streamflow increased

during the spring and winter months and decreased for the summer months for all time periods and emission scenarios. For Rush Creek, average monthly streamflow increased for the late winter and spring months, decreased during the summer months, and had no apparent trend for the early winter months for all time periods and emission scenarios. For the 2050s, the largest increase occurred in April for Lee Vining Creek (60 % increase) and March for Rush Creek (60 % increase). The largest monthly streamflow decrease for the 2050s occurred in July for both creeks with a 35 % decrease for Lee Vining and Rush Creeks. The largest average monthly streamflow increase for the 2080s occurred in March for Lee Vining (100 % increase) and Rush Creek (120 % increase). The largest decrease for the 2080s occurred in July for Lee Vining (50 % decrease) and Rush Creek (55 % decrease).

3.4 Probability of future 'wet' and 'dry' hydrologic years in the Mono Lake Basin

While projected temperature and precipitation changes will likely have serious implications for streamflow timing, the distribution of 'wet' and 'dry' hydrologic years will also shift (Table 5). Figure 9 displays percent exceedance curves of historical and future streamflows along with the established 'wet' and 'dry' year streamflows shown in Table 3. From this we can determine how the 'wet' and 'dry 'distributions can be expected to shift under climate change. As previously noted, by legal mandate the amount of water diverted out of MLB is contingent on whether the previous hydrologic year is 'wet' or 'dry' based on the definition in Section 2.5. The annual streamflow median value, as well as the 1st (25th percentile; not

Table 5 Percent exceedances based on established 'wet' and 'dry' year streamflow values. All values are in percent

	Time Period	Median	3rd Quartile	1st Quartile
Wet hydrologic years				
Lee Vining	Historical Ave.	25	–	–
B1	2050s	11	13	5
	2080s	9	14	5
A2	2050s	17	33	12
	2080s	13	30	4
Rush	Historical Ave.	23	–	–
B1	2050s	12	16	7
	2080s	10	15	8
A2	2050s	12	27	10
	2080s	10	25	2
Dry hydrologic years				
Lee Vining	Historical Ave.	93	–	–
B1	2050s	91	96	88
	2080s	89	92	81
A2	2050s	86	96	83
	2080s	80	91	75
Rush	Historical Ave.	83	–	–
B1	2050s	74	85	66
	2080s	72	84	64
A2	2050s	72	88	68
	2080s	58	80	55

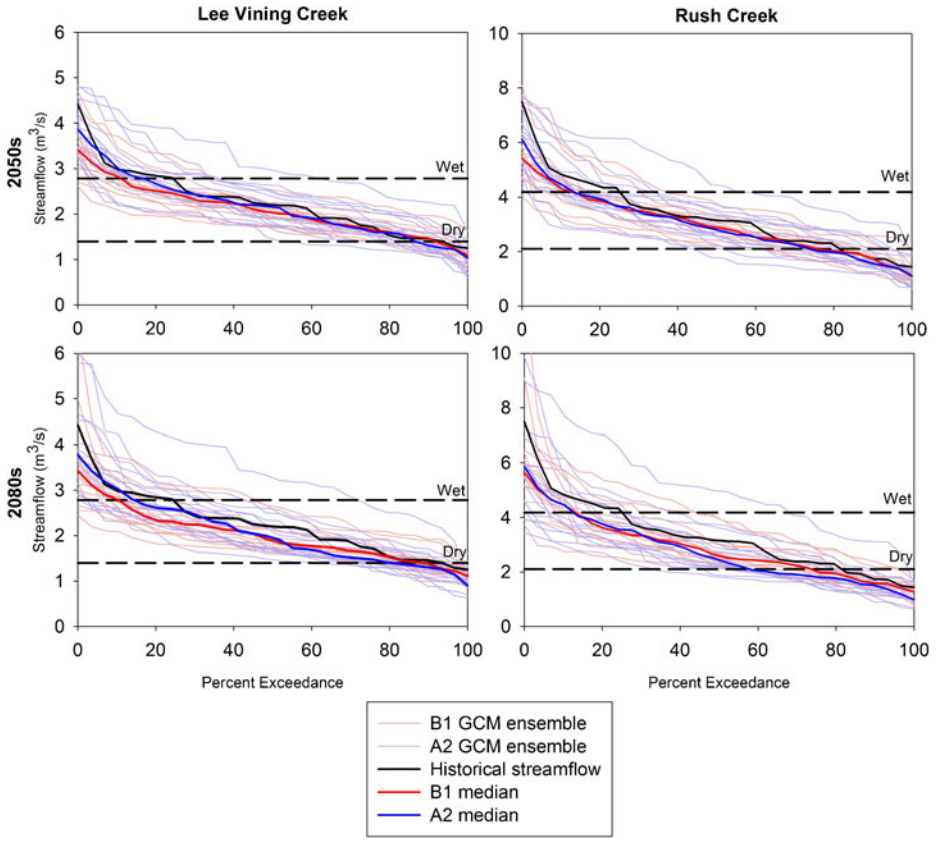

Fig. 9 Percent exceedance plots based on the California Supreme Court 'wet' and 'dry' year definitions for all emission scenarios and time periods

shown in Fig. 9) and 3rd quartiles (75th percentile; not shown in Fig. 9), for the GCM ensemble are assessed.

For both creeks, the occurrence of 'wet' hydrologic years will decrease in the 2050s under either emission scenario. At the Lee Vining outlet, during the historical time period, a 'wet' hydrologic year streamflow value is exceeded approximately 25 % of the time (Fig. 9). In the 2050's, the median exceedance of this value will decrease to 11 % for the B1 scenario and 17 % for the A2 scenario. For the 1st quartile, the 'wet' hydrologic streamflow value is exceeded 5 % of the time under the B1 scenario and 12 % under the A2 scenario. For the 3rd quartile, the 'wet' streamflow value is exceeded 13 % of the time under the B1 scenario and 33 % under the A2 scenario. Thus, only the 3rd quartile under the A2 scenario displays an increase in 'wet' hydrologic years. During the 2080s, the median percent further decreases to 9 % for the B1 scenario and 13 % under the A2 scenario. The occurrence of 'wet' hydrologic years for the 1st quartile further decreases to 5 % under the B1 scenario and 4 % for the A2 scenario during the 2080s. For the 3rd quartile, the 'wet' hydrologic year streamflow value is exceeded 14 % under the emission scenario and 30 % under the A2 scenario. Again, only the 3rd quartile A2 scenario value exceeds the historical value for "wet" hydrologic years.

The occurrence of 'wet' hydrologic years also decreases for Rush Creek. During the historical time period, a 'wet' hydrologic year streamflow value is exceeded

approximately 23 % of the time. The B1 and A2 emission scenarios show similar percent decreases to approximately 12 % for the 2050s and 10 % for the 2080s (median values). During the 2050s, under the B1 scenario, the 1st and 3rd quartile percent exceedances are 7 and 16 %, respectively. The 1st and 3rd quartiles are 10 and 27 %, respectively, under the A2 scenario. During the 2080s, under the B1 scenario, the 1st and 3rd quartile percent exceedance values are 8 and 15 %, respectively, and 2 and 25 % under the A2 scenario. As found for Lee Vining creek, the 3rd quartile for both emission scenarios is the only value that exceeds the historical value for the occurrence of 'wet' hydrologic years.

Further, our results suggest an increase in the occurrence of drought years with projected climatic changes in the MLB (Fig. 9). Under current climatic conditions, median streamflow is higher than the 'dry' streamflow value approximately 93 % of the time for Lee Vining Creek, thus drought years occur 7 % of the time. During the 2050s, this value shifts to 91 % for the B1 scenario and 86 % for the A2 scenario. For the 1st quartile, the 'dry' hydrologic streamflow value is exceeded 88 % of the time under the B1 scenario and 83 % under the A2 scenario. The 3rd quartile is exceeded 96 % of the time for both scenarios. The median 'dry' streamflow exceedance further shifts during the 2080s to 89 % for B1 scenario and 80 % for the A2 scenario. Thus, late in the study period, the median occurrence of drought years would increase to 11 % and 20 % for the B1 and A2 scenarios, respectively. For the 2080s, the exceedance of 'dry' hydrologic years for the 1st quartile is 81 % under the B1 scenario and 75 % under the A2 scenario. For the 3rd quartile, the 'dry' hydrologic year streamflow value is exceeded 92 % under the emission scenario and 91 % under the A2 scenario.

For Rush Creek, droughts conditions are even more likely. Under current climatic conditions, the 'dry' streamflow value is exceeded approximately 83 % of the time. The median value shifts during the 2050s to 74 % for the B1 scenario and 72 % for the A2 scenario. During the 2050s, under the B1 scenario, the 1st and 3rd quartile percent exceedances were 66 and 85 %, respectively. These values slightly increase under the A2 scenario, where the 1st and 3rd quartile values are 68 and 88 %, respectively. During the 2080s, the 'dry' streamflow value is only exceeded 72 % of the time for the B1 scenario and 58 % for the A2 scenario, suggesting that drought conditions will likely occur in 28 % and 42 % of the years for the B1 and A2 scenarios. During the 2080s, under the B1 scenario, the 1st and 3rd quartile percent exceedance values are 64 and 84 %, respectively, and 55 and 80 % under the A2 scenario. Thus, for both inflows, the median and 1st quartile during the 2050's and 2080s are in agreement that the occurrence of 'dry' hydrologic years will increase, while the 3rd quartile values for drought exceedance are very close to historical conditions.

4 Implications and conclusions

Mono Lake in the California Sierra Nevada represents a unique ecosystem that has been affected by water diversions to the City of Los Angeles over several decades, and has been the subject of a landmark ruling recognizing the application of the public trust doctrine and guaranteeing minimum flows to the lake. This study assessed the impacts of projected climatic change through the end of the century on the inflows to MLB using the SWAT hydrologic model. The inflows considered here are Lee Vining and Rush creeks, as they represent important sources for water diversions by the LADWP. The model was calibrated and validated with historical natural monthly streamflow data from the CA DWR, and was able to satisfactorily replicate the streamflow, with NS coefficients of about 0.8 for calibration and validation in both creeks. Subsequently, output from 16 different GCMs and for the B1 and A2 emission scenarios was used to drive the hydrologic model.

Based on the 16 GCM projections, climate in the MLB was affected such that temperature (and hence evapotranspiration) appreciably increased, while overall precipitation saw little or no change. Annual average increases in temperature by the end of the century are 2.5 and 4.1 °C for the B1 and A2 emission scenarios, respectively. The GCM ensemble predicts a decrease in average change in annual precipitation by 3 % for the B1 scenario and 1.7 % for the A2 scenario by the end of the century.

Our modeling results suggest that annual streamflow rates will decrease for both creeks, with the largest declines by the end of the century. The decreased flows were observed in spite of very small changes in precipitation amounts and can be explained by higher land evapoptranspiration rates. The average annual total land evapotranspiration is project to increase by 10 mm by the end of the century for both emission scenarios. Decreases in average annual streamflow, as indicated in this study, will lead to less water available for aquatic ecosystems and water resources. Decreases in streamflow coupled with increases in Mono Lake evaporation from increased temperatures will further reduce the Mono Lake volume (Schneider et al. 2009).

In addition to reduced overall streamflow, warmer temperatures connected to decreased snow deposition and earlier snowmelt are expected to shift the timing of the spring snowmelt runoff to earlier in the year. Peak runoff in the MLB historically occurred in June, but could advance to earlier in June, and May for the B1 and A2 emission scenarios, respectively, by 2050. For the 2080s, under both emission scenarios, the peak will advance from June to May. The magnitude and direction of this projected shift is similar to that of other studies for the Western United States (Stewart et al. 2005). Changes in flow timing could have serious implications for ecosystems and water diversions connected to the Mono Lake inflows, both of which depend on certain seasonal flows. In addition, the in-stream requirements for Lee Vining and Rush Creeks differ between the Spring and Summer months (April through September) and Fall and Winter months (October through March). Our results showed that shifts in streamflow timing are likely to increase the Fall and Winter streamflow average, while concurrently decreasing the Spring and Summer month average. Specifically, the earlier snowmelt peak resulted in decreased modeled summer flows, a time of year when water usage demand is at its highest, thus further complicating water resource diversions.

While climate change is expected to have serious implications for streamflow amounts and timing, it will likely also affect the distribution of ‘wet’, ‘normal’, and ‘dry’ years, as currently defined by the California Supreme Court for the purpose of water diversions. The ‘dry’, ‘normal’ and ‘wet’ year designations for any given year determine the minimum in-stream flow requirements for the following year and are a thus a critical component for both maintaining aquatic ecosystems and municipal water resources. Based on the 1983 California Supreme Court decision, the LADWP can divert more water out of MLB when ‘wet’ or ‘normal’ hydrologic years occur. Our results, given as the number of years in which flow exceeds the ‘dry’ or ‘wet’ cutoffs, indicate a substantial increase in the occurrence of ‘dry’ years and a decrease of ‘wet’ years by the end of the century. Assuming that all other conditions remain the same, an increased occurrence of drought conditions could cause significant changes in the sustainability of water resources within MLB. Less available water leaves water managers with one of two options: Either the water left in the system for ecosystem sustenance will be removed, or water deliveries to southern California will become less reliable, especially as the 1983 California Supreme Court decision generally sided with the health of the ecosystem and lake.

Because of its unique ecosystem, expansive water resource history and controversy, and pivotal role in the history of environmental legislation, an assessment of the effect of climatic changes on the MLB water resources is of special importance. While our modeling

results suggest important climate induced hydrologic changes in the MLB, it should be noted, that many other factors that will influence future streamflow, such as land use, vegetation, geomorphic and population changes, are not accounted for in this study. Larger populations and longer growing seasons due to warming temperatures may drive the system further towards conditions of less available streamflow.

Acknowledgments The authors gratefully acknowledge financial support for this work from the U.S. Environmental Protection Agency through EPA STAR Grant No. RD-83419101-0. We acknowledge the modeling groups, the Program for Climate Model Diagnosis and Intercomparison (PCMDI) and the WCRP's Working Group on Coupled Modelling (WGCM) for their roles in making available the WCRP CMIP3 multi-model dataset. Support of this dataset is provided by the Office of Science, U.S. Department of Energy.

References

Abbaspour KC, Yang J, Maximov I, Siber R, Bogner K, Mieleitner J, Zobrist J, Srinivasan R (2007) Modelling hydrology and water quality in the pre-alpine/alpine Thur watershed using SWAT. J Hydrol 333:413–430

Arnold JG, Srinivasan R, Muttiah RS, Williams JR (1998) Large area hydrologic modeling and assessment Part 1: model development. J Am Water Resour Assoc 34:73–89

Barnett TP, Pierce DW, Hidalgo HG, Bonfils C, Santer BD, Das T, Bala G, Wood AW, Nozawa T, Mirlin AA, Cayan DR, Dettinger MD (2008) Human-induced changes in hydrology of the Western United States. Science 319(5866):1080–1083

Blumm M, Schwartz T (2003) Mono Lake and Evolving Public Trust in Western Water. Issues in Legal Scholarship

Cayan DR, Maurer EP, Dettinger MD, Tyree M, Hayhoe K (2008) Climate change scenarios for the California region. Clim Change 87:21–42

Collins WD, Bitz CM, Blackmon ML, Bonan GB, Bretherton CS, Carton JA, Chang P, Doney SC, Hack JJ, Henderson TB, Kiehl JT, Large WG, McKenna DS, Santer BD, Smith RD (2006) The Community Climate System Model: CCSM3. J Clim 19:2122–2143

Dana GL, Lenz PH (1986) Effects of increasing salinity on an Artemia population from Mono Lake, California. Oecologia 68:428–436

Delworth TL, Broccoli AJ, Rosati A, Stouffer RJ, Balaji V, Beesley JA, Cooke WF, Dixon KW, Dunne J, Dunne KA, Durachta JW, Findell KL, Ginoux P, Gnanadesikan A, Gordon CT, Griffies SM, Gudgel R, Harrison MJ, Held IM, Hemler RS, Horowitz LW, Klein SA, Knutson TR, Kushner PJ, Langenhorst AR, Lee H-C, Lin S-J, Lu J, Malyshev SL, Milly PCD, Ramaswamy V, Russell J, Schwarzkopf MD, Shevliakova E, Sirutis JJ, Spelman MJ, Stern WF, Winton M, Wittenberg AT, Wyman B, Zeng F, Zhang R (2006) GFDL's CM2 global coupled climate models - Part 1: formulation and simulation characteristics. J Clim 19:643–674

Diansky NA, Volodin EM (2002) Simulation of present-day climate with a coupled Atmosphere–ocean general circulation model. Izv Atmos Ocean Phys (Engl Transl) 38:732–747

Flato GM, Boer GJ (2001) Warming asymmetry in climate change simulations. Geophys Res Lett 28:195–198

Fontaine TA, Cruickshank TS, Arnold JG, Hotchkiss RH (2002) Development of a snowfall-snowmelt routine for mountainous terrain for the soil and water assessment tool (SWAT). J Hydrol 262:209–223

Furevik T, Bentsen M, Drange H, Kindem IKT, Kvamstø NG (2003) Description and evaluation of the bergen climate model: ARPEGE coupled with MICOM. Clim Dyn 21:27–51

Gassman PW, Reyes MR, Green CH, Arnold JG (2007) The soil and water assessment tool: historical development, applications, and future research directions. Trans ASABE 50:1211–1250

Gordon C, Cooper C, Senior CA, Banks H, Gregory JM, Johns TC, Mitchell JFB, Wood RA (2000) The simulation of SST, sea ice extents and ocean heat transports in a version of the Hadley Centre coupled model without flux adjustments. Clim Dyn 16:147–168

Gordon HB, Rotstayn LD, McGregor JL, Dix MR, Kowalczyk EA, O'Farrell SP, Waterman LJ, Hirst AC, Wilson SG, Collier MA, Watterson IG, Elliott TI (2002) The CSIRO Mk3 climate system model, CSIRO Atmospheric Research Technical Paper No.60. CSIRO. Division of Atmospheric Research, Victoria, p 130

Hawkins E, Sutton R (2009) The potential to narrow uncertainty in regional climate predictions. Bul Am Meterol Soc 90:1095–1107

Hawkins E, Sutton R (2010) The potential to narrow uncertainty in projections of regional precipitation change. ClimvDyn 37:407–418

IPSL (2005) The new IPSL climate system model: IPSL-CM4. Institut Pierre Simon Laplace des Sciences de l'Environnement Global, Paris, p 73

Jungclaus JH, Botzet M, Haak H, Keenlyside N, Luo J-J, Latif M, Marotzke J, Mikolajewicz U, Roeckner E (2006) Ocean circulation and tropical variability in the AOGCM ECHAM5/MPI-OM. J Clim 19:3952–3972

K-1 model developers (2004) K-1 coupled model (MIROC) description', K-1 technical report, 1. In: Hasumi H, Emori S (eds) Center for climate system research. University of Tokyo, Tokyo, p 34

Karl TR, Riebsame WE (1984) The Identification of 10- to 20-Year Temperature and Precipitation Fluctuations in the Contiguous United States. J Clim Appl Meteorol 23:950–966

Krause P, Boyle DP, Bäse F (2005) Comparison of different efficiency criteria for hydrological model assessment. Adv Geo 5:89–97

LADWP (1995) LADWP draft stream restoration plan. LADWP, Los Angeles

Legutke S, Voss R (1999) The Hamburg atmosphere–ocean coupled circulation model ECHO-G, Technical report, No. 18. German Climate Computer Centre (DKRZ), Hamburg, p 62

Lobell DB, Field CB, Cahill KN, Bonfils C (2006) Impacts of future climate change on California perennial crop yields: Model projections with climate and crop uncertainties. Agrl For Meteorol 141:208–218

Loomis JB (1987) Balancing public trust resources of Mono Lake and Los Angeles' Water Right: An economic approach. Water Resour Res 23:1449–1456

Maurer EP (2007) Uncertainty in Hydrologic Impacts of Climate Change in the Sierra Nevada, California Under Two Emissions Scenarios. Climatic Change 82:309–325. doi:10.1007/s10584-006-9180-9

Maurer EP, Wood AW, Adam JC, Lettenmaier DP, Nijssen B (2002) A long-term hydrologically-based data set of land surface fluxes and states for the conterminous United States. J Clim 15:3237–3251

Maurer EP, Hidalgo HG, Das T, Dettinger MD, Cayan DR (2010) The utility of daily large-scale climate data in the assessment of climate change impacts on daily streamflow in California. Hyd Earth Sys Sci 14:1125–1138

Meehl GA, Covey C, Delworth T, Latif M, McAvaney B, Mitchell JFB, Stouffer RJ, Taylor KE (2007a) The WCRP CMIP3 multimodel dataset: a new era in climate change research. Bul Am Meterol Soc 88:1383–1394

Meehl GA et al (2007b) Global climate projections. In: Solomon S, Qin D, Manning M, Chen Z, Marquis M, Averyt KB, Tignor M, Miller HL (eds) The physical science basis. Contribution of Working Group I to the fourth assessment report of the intergovernmental panel on climate change. Cambridge University Press, Cambridge, pp 747–846

Mono Basin Environmental Impact Report (Mono Basin EIR) (1993) Final environmental impact report for the review of Mono Basin water rights of the city of Los Angeles. California State Water Resources Control Board, Sacramento

Monteith JIL (1965) Evaporation and environment. Academic, NY

Moriasi DN, Arnold JG, Liew MWV, Bingner RL, Harmel RD, Veith TL (2007) Model evaluation guidelines for systematic quantification of accuracy in watershed simulations. Trans ASABE 50:885–900

Neitsch SL, Arnold JG, Kiniry JR, Williams JR, King KW (2005) Soil and water assessment tool theoretical documentation: version 2005. Texas Water Resources Institute, College Station

Penman HL (1956) Evaporation: an introductory survey. Neth J Agric Sci 1:9–29, 87–97, 151–153

Roe GH, Baker MB (2007) Why is climate sensitivity so unpredictable? Science 318:629–632

Russell GL, Rind D (1999) Response to CO2 transient increase in the GISS coupled model: regional coolings in a warming climate. J Clim 12:531–539

Russell GL, Miller JR, Rind D, Ruedy RA, Schmidt GA, Sheth S (2000) Comparison of model and observed regional temperature changes during the past 40 years. J Geophys Res-Atmos 105:14891–14898

Salas-Mélia D, Chauvin F, Déqué M, Douville H, Gueremy JF, Marquet P, Planton S, Royer JF, Tyteca S (2005) Description and validation of the CNRM-CM3 global coupled model, CNRM working note 103. Centre National de Recherches Météorologiques, Météo-France, Toulouse, p 36

Sanderson BM, Piani C, Ingram WJ, Stone DS, Allen MR (2007) Towards constraining climate sensitivity by linear analysis of feedback patterns in thousands of perturbed-physics GCM Simulations. Clim Dyn 30:175–190

Schneider P, Hook SJ, Radocinksi RG, Corlett GK, Hulley GC, Schladow SG, Steissberg TE (2009) Satellite observations indicate rapid warming trend for lakes in California and Nevada. Geophys Res Lett 36:L22402

Steinhart P (1980) The city and the inland sea. Audubon, 98–125

Stewart IT, Cayan DR, Dettinger MD (2005) Changes toward earlier streamflow timing across western North America. J Clim 18:1136–1155

US Fish and Wildlife Service (USFWS) (2006) Endangered and Threatened Wildlife and Plants; 90-Day Finding on Petitions to List the Mono Basin Area Population of the Greater Sage-Grouse as Threatened or Endangered. In: United States Fish and Wildlife Service, Department of the Interior, Washington D.C

USDA (1972) National Engineering Handbook: Hydrology. In: Agriculture. U.S. Government Print Office, Washington D.C

Vorster P (1985) A water balance forecast model for Mono Lake, California. M.S. Thesis. Geography Department. California State University, Hayward

Washington WM, Weatherly JW, Meehl GA, Semtner AJ, Bettge TW, Craig AP, Strand WG, Arblaster J, Wayland VB, James R, Zhang Y (2000) Parallel climate model (PCM) control and transient simulations. Clim Dyn 16:755–774

Western Regional Climate Center (WRCC) (2011) Long-term climate data for Mono Lake, California. http://www.wrcc.dri.edu/cgi-bin/cliMAIN.pl?camono+nca. Accessed 1/14/2011

Wigley TML, Jones PD (1985) Influences of precipitation changes and direct CO_2 effects on streamflow. Nature 314:149–152

Wood AW, Maurer EP, Kumar A, Lettenmaier DP (2002) Long-range experimental hydrologic forecasting for the eastern United States. J Geophys Res 107:4429

Wood AW, Leung LR, Sridhar V, Lettenmaier DP (2004) Hydrologic implications of dynamical and statistical approaches to downscaling climate model outputs. Clim Change 62:189–216

Yukimoto S, Noda A, Kitoh A, Sugi M, Kitamura Y, Hosaka M, Shibata K, Maeda S, Uchiyama T (2001) The new Meteorological Research Institute coupled GCM (MRI-CGCM2), Model climate and variability. Pap Meteorol Geophys 51:47–88